

Supporting Information

for *Laser Photonics Rev.*, DOI 10.1002/lpor.202401938

mrPCA-PSP: Robust Motion-Resistant Phase-Shifting Profilometry Based on Principal Component Analysis

Yixuan Li, Mingzheng Li, Wenwu Chen, Jiaming Qian, Shijie Feng*, Qian Chen* and Chao Zuo**

Supplementary Information for mrPCA-PSP: Robust motion-resistant phase-shifting profilometry based on principal component analysis

Yixuan Li^{1,2,3,4}, Mingzheng Li^{1,2,3,4}, Wenwu Chen^{1,2,3}, Jiaming Qian^{1,2,3,*}, Shijie Feng^{1,2,3,*},
Qian Chen^{1,2,3,*}, and Chao Zuo^{1,2,3,*}

¹Smart Computational Imaging (SCI) Laboratory, Nanjing University of Science and Technology, Nanjing, Jiangsu Province 210094, China

²Smart Computational Imaging Research Institute (SCIRI) of Nanjing University of Science and Technology, Nanjing, Jiangsu Province 210094, China

³Jiangsu Key Laboratory of Spectral Imaging & Intelligent Sense, Nanjing University of Science and Technology, Nanjing, Jiangsu Province 210094, China

⁴These authors contributed equally to this work.

*jiaming_qian@njust.edu.cn

*shijiefeng@njust.edu.cn

*chenqian@njust.edu.cn

*zuochao@njust.edu.cn

ABSTRACT

This document provides supplementary information for “mrPCA-PSP: Robust motion-resistant phase-shifting profilometry based on principal component analysis”. We present the configuration of the hardware system and the selection of the optimal fringe frequency, and verify the robustness and advantages of mrPCA-PSP.

Contents

Supplementary Note S1. Hardware system configuration and fringe frequency selection

Supplementary Note S2. Accuracy and robustness of mrPCA-PSP at different motion speeds

Supplementary Note S3. Comparative analysis of phase demodulation methods

Supplementary Note S4. Performance evaluation of mrPCA-PSP in dynamic measurement scenarios

Supplementary Note S1. Hardware system configuration and fringe frequency selection

The system comprises a digital light processing (DLP) projector (LightCrafter 4500 Pro) with a resolution of 912×1140 pixels and three monochrome cameras (Basler acA640-750um), each with a resolution of 640×480 pixels. The projector continuously projects three-step phase-shifted fringe patterns and synchronously triggers the cameras to capture images at a rate of 100 frames per second (fps), and the exposure time of the cameras is set to 8500 us. The projected fringe patterns have 64 periods, and the system's working distance from the object is approximately 1 m. The size of the view field is $250\text{mm} \times 200\text{mm}$, and the measurable depth range is 400mm. For absolute phase retrieval, we employ a stereo phase unwrapping algorithm based on multi-view geometric constraints. High-frequency fringes provide more detailed surface information, but increase the difficulty of phase unwrapping.

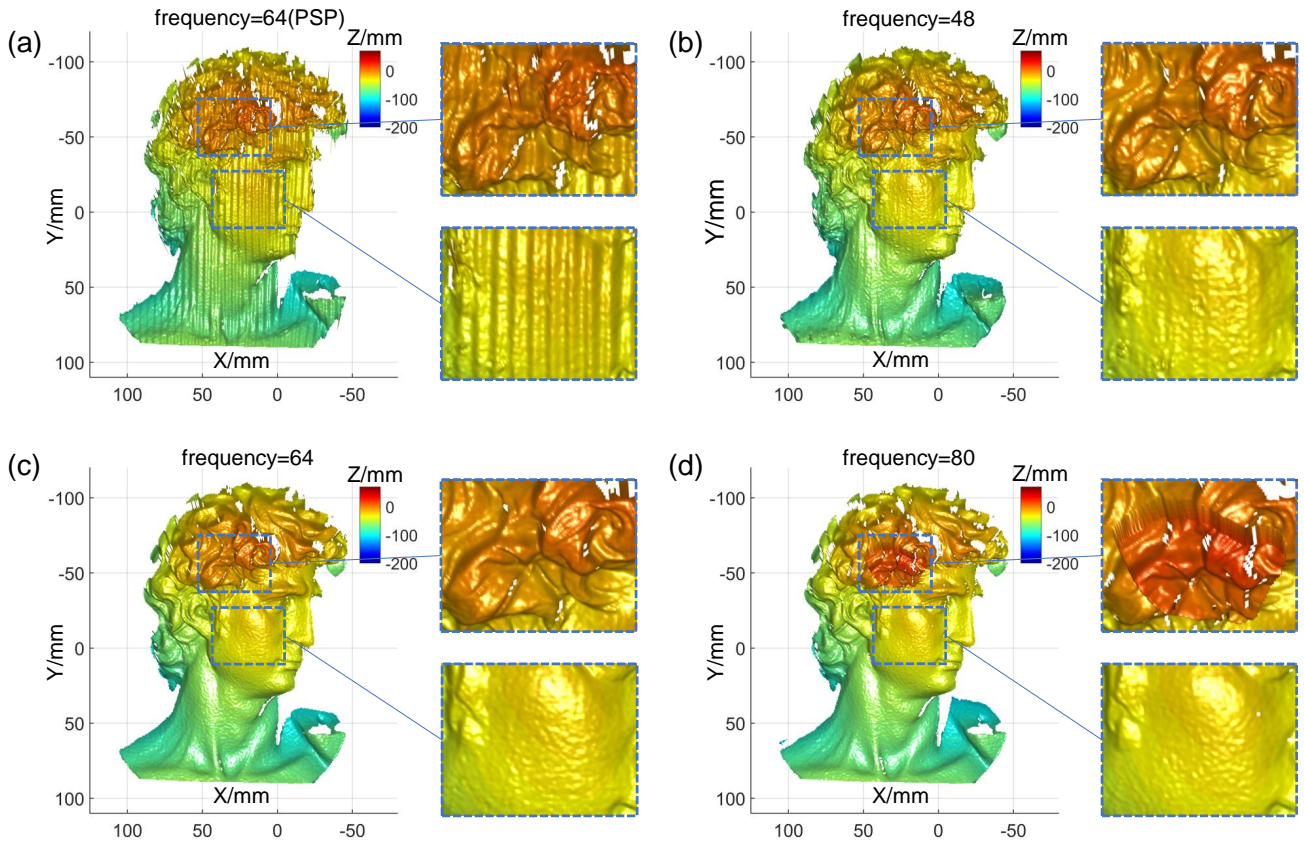


Figure S1. Reconstructed results with different frequencies: (a) Reconstructed result using PSP with a frequency of 64, (b, c, d) Reconstructed results using mrPCA-PSP with frequencies of 48, 64, 80.

The selection of fringe frequency is critical for accurate phase retrieval and phase unwrapping in our method. Several factors must be considered to achieve an optimal balance between measurement accuracy and robustness. Although higher fringe frequencies improve phase measurement accuracy and capture finer

3D details, they also introduce phase ambiguity and unwrapping errors. Additionally, high frequencies can amplify noise and increase susceptibility to motion-induced artifacts and defocusing. The chosen frequency must also be compatible with the field of view, depth of field, and spatial resolution of the projector-camera system to prevent aliasing and undersampling effects. In our approach, each phase-shifted image contains distinct phase offsets beyond simple image translation. To reduce the influence of fringe modulation on the phase correlation algorithm, we use a windowing function to isolate only the DC component. This requires a fringe frequency that is high enough to avoid spectral aliasing between the zero frequency and the fundamental frequency while preventing phase unwrapping errors. To further investigate the impact of fringe frequency on phase retrieval accuracy and motion compensation, we conducted additional experiments with fringe frequencies of 48, 64, and 80 periods. Figure S1 shows the reconstructed results under these different frequencies in a dynamic scene, demonstrating the influence of frequency selection on measurement accuracy and surface quality. In Fig. S1(a), a traditional phase-shifting profilometry (PSP) method with a fringe period of 64 (used as a reference) produces a reconstruction with noticeable motion ripples. Figures S1(b), (c), and (d) present the reconstructions and corresponding zoomed-in views obtained using the mrPCA-PSP method with frequencies of 48, 64, and 80, respectively. When the frequency is relatively low (i.e., $f=48$, Fig. S1(b)), the compensation performance degrades, resulting in a rough reconstructed surface; when the frequency is set higher (i.e., $f=80$, Fig. S1(d)), depth estimation errors appear. By contrast, the mrPCA-PSP approach with a frequency of 64 (Fig. S1(c)) achieves high-quality reconstructions after compensation, avoiding phase-unwrapping errors caused by excessively high frequencies. These results confirm that, under our system configuration, a fringe frequency of 64 provides the best balance between measurement sensitivity, phase stability, and robustness against motion errors, thereby minimizing aliasing and preventing phase unwrapping problems for accurate and reliable reconstructions in dynamic measurement scenarios.

Supplementary Note S2. Accuracy and robustness of mrPCA-PSP at different motion speeds

In order to verify that the motion speed does not significantly affect the compensated measurement results, we further tested the dynamic measurement accuracy at different speeds. Figure S2 shows the root mean square (RMS) errors of the tested algorithms when measuring a standard ceramic sphere moving at various speeds (0 to 100 mm/s, in increments of 20 mm/s). We employed the same system configuration described in the main text, with a 100 fps projector, 8500 us camera exposure time, and a fringe period of 64. As depicted in Fig. S1, the RMS errors are smallest when the object is stationary; however, the overall measurement accuracy remains stable even as the speed increases. Among the tested algorithms, our mrPCA-based approach consistently demonstrates the lowest RMS errors across the entire speed range, confirming its robustness and adaptability to dynamic conditions. These findings suggest that for this particular hardware setup, object velocities of up to 100 mm/s can be accommodated without significantly compromising measurement precision.

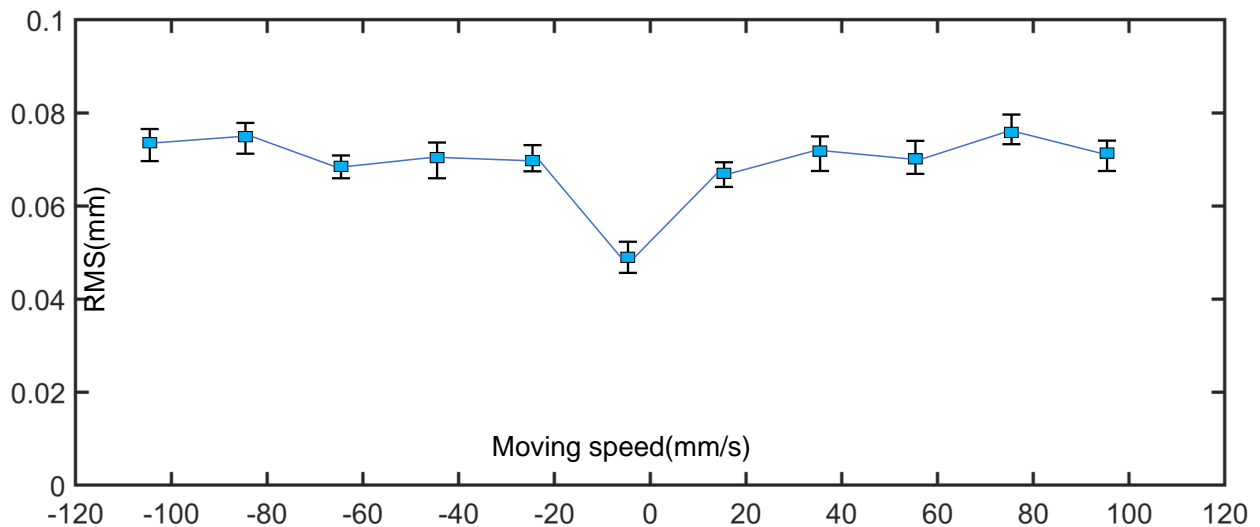


Figure S2. The RMS errors at different moving speed.

Supplementary Note S3. Comparative analysis of phase demodulation methods

In order to show more intuitively the advantage of the proposed method in phase error reduction, we measured a plaster statue at three different positions and took the i -th fringe image of the i -th position ($i = 1, 2, 3$) to simulate the motion. The phase map of the first position is used as the standard value to obtain the phase error maps under different methods. Fig. S3 demonstrates the error compensation performance of different methods, Fig. S3(a-f) shows the phase error maps of PSP¹, Lu's method², Weise's method³, Wang's method⁴, Wu's method⁵ and mrPCA-PSP, respectively, and the MAE of phase error is 0.1856rad, 0.1215rad, 0.1208 rad, 0.1388 rad, 0.1074 rad and 0.0611 rad. From the experimental results, it can be seen that mrPCA-PSP is able to minimize the phase error caused by motion compared to other motion error compensation methods, which reflects the advantages of mrPCA-PSP in motion compensation.

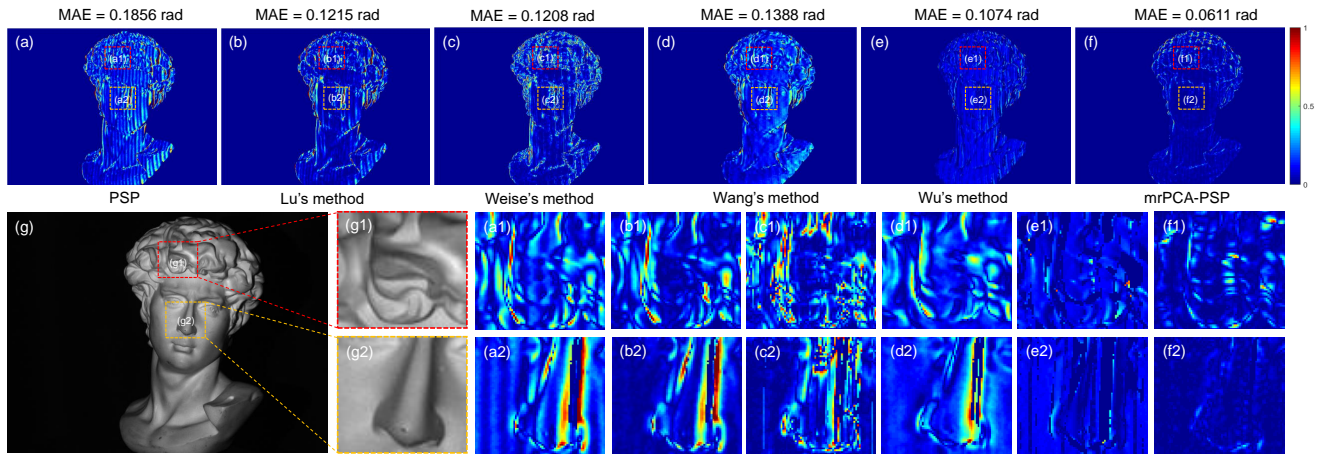


Figure S3. Comparison of phase errors across different methods. Calculated phase error results for (a) PSP, (b) Lu's method, (c) Weise's method, (d) Wang's method, (e) Wu's method, (f) mrPCA-PSP. (g) A photograph of the test plaster statue of David. (a1-g1, a2-g2) Magnified views of two selected complex regions for detailed analysis.

Supplementary Note S4. Performance evaluation of mrPCA-PSP in dynamic measurement scenarios

Since the mrPCA-PSP method estimates and compensates for the translation of the entire fringe image, it assumes that all objects within the image move in the same way. To handle multiple objects with different motions, we incorporate a segmentation algorithm⁶ to separate isolated objects before applying motion compensation. To verify the performance of our method in such scenarios, we tested a scene containing two isolated objects: a stationary plaster statue of an angel girl and a moving hand. The measurement results are presented in Fig. S4. Figure S4(b) and (e) show the 3D reconstructions before motion compensation at different time frames, while Fig. S4(c) and (f) display the results after applying mrPCA-PSP. The comparison, also shown in [Visualization S1](#), demonstrates that our method can effectively process objects with different motion states separately, significantly reducing motion-induced errors.

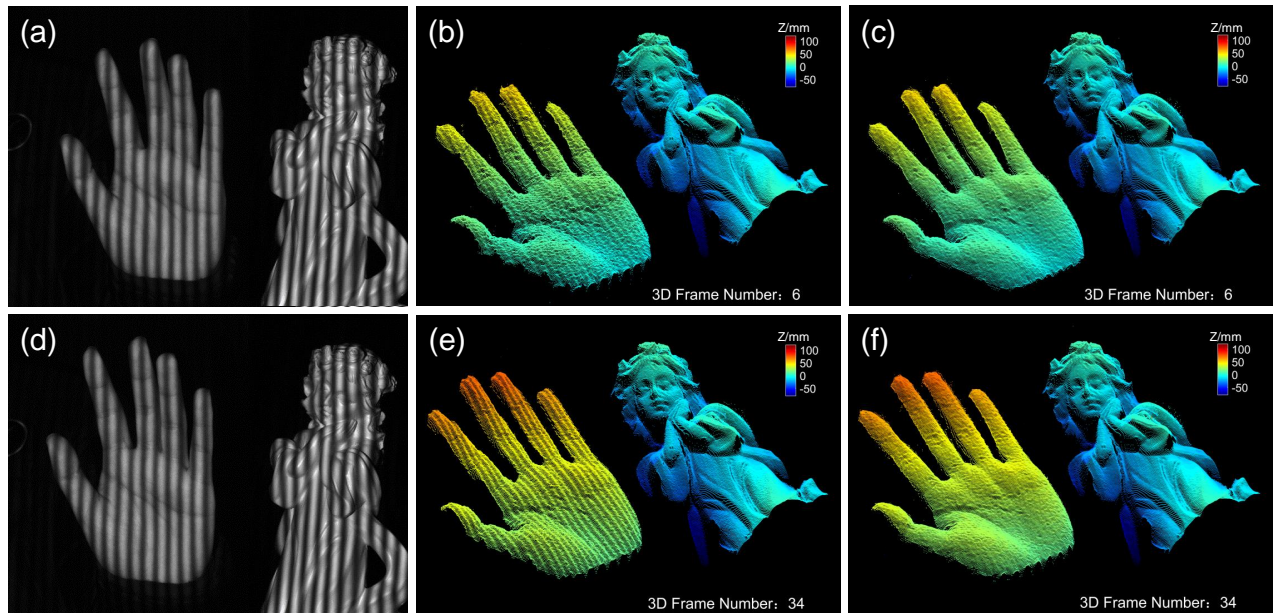


Figure S4. Measurement results of two isolated objects in different motion states. (a), (d) Captured fringe images at different frames, showing a stationary plaster statue of an angel girl and a moving hand. (b), (e) Reconstructed results before motion compensation, illustrating significant motion-induced artifacts on the moving object. (c), (f) Reconstructed results after applying the proposed mrPCA-PSP method, effectively reducing motion-induced errors and accurately capturing both stationary and moving objects. ([Visualization S1](#))

References

1. Zuo, C. *et al.* Phase shifting algorithms for fringe projection profilometry: A review. *Opt. lasers engineering* **109**, 23–59 (2018).
2. Lu, L., Xi, J., Yu, Y. & Guo, Q. Improving the accuracy performance of phase-shifting profilometry for the measurement of objects in motion. *Opt. letters* **39**, 6715–8 (2014).
3. Weise, T., Leibe, B. & Van Gool, L. Fast 3d scanning with automatic motion compensation. In *2007 IEEE Conference on Computer Vision and Pattern Recognition*, 1–8 (IEEE, 2007).
4. Wang, Y., Liu, Z., Jiang, C. & Zhang, S. Motion induced phase error reduction using a hilbert transform. *Opt. Express* **26**, 34224–34235 (2018).
5. Wu, G., Yang, T., Liu, F. & Qian, K. Suppressing motion-induced phase error by using equal-step phase-shifting algorithms in fringe projection profilometry. *Opt. Express* **30**, 17980–17998 (2022).
6. Feng, S. *et al.* Robust dynamic 3-d measurements with motion-compensated phase-shifting profilometry. *Opt. Lasers Eng.* **103**, 127–138 (2018).